0022-3565/10/3322-562–568$20.00
THE JOURNAL OF PHARMACOLOGY AND EXPERIMENTAL THERAPEUTICS
JPET 332:562–568, 2010

Vol. 332, No. 2
161893/3550697
Printed in U.S.A.

Quantitative Prediction and Clinical Observation of a CYP3A Inhibitor-Based Drug-Drug Interactions with MLN3897, a Potent C-C Chemokine Receptor-1 Antagonist

Chuang Lu, Suresh K. Balani, Mark G. Qian, Shimoga R. Prakash, Patricia S. Ducray, and Lisa L. von Moltke

Drug Metabolism and Pharmacokinetics (C.L., S.K.B., M.G.Q., S.R.P.) and Clinical Pharmacology (P.S.D., L.L.v.M.), Millennium Pharmaceuticals, Inc., Cambridge, Massachusetts

Received September 21, 2009; accepted November 2, 2009

ABSTRACT

A novel in vitro model was recently developed in our laboratories for the prediction of magnitude of clinical pharmacokinetic drug-drug interactions (DDIs), based on reversible hepatic cytochrome P450 (P450) inhibition. This approach, using inhibition data from human hepatocytes incubated in human plasma, and quantitative P450 phenotyping data from hepatic microsomal incubations, successfully predicted DDIs for 15 marketed drugs with ketoconazole, a strong competitive inhibitor of CYP3A4/5, generally used to demonstrate a "worst-case scenario" for CYP3A inhibition. In addition, this approach was successfully extended to DDI predictions with the moderate competitive CYP3A inhibitor fluconazole for nine marketed drugs. In the current report, the general applicability of the model has been demonstrated by prospectively predicting the degree of inhibition and then conducting DDI studies in the clinic for an investigational CCR1 antagonist MLN3897, which is cleared predominantly by CYP3A. The clinical studies involved treatment of healthy volunteers (n = 17–20), in a crossover design, with ketoconazole (200 mg b.i.d.) or fluconazole (400 mg once a day), while receiving MLN3897. Administration of MLN3897 and ketoconazole led to an average 8.28-fold increase in area under the curve of plasma concentration-time plot (AUC) of MLN3897 at steady state, compared with the 8.33-fold increase predicted from the in vitro data. Similarly for fluconazole, an average increase of 3.93-fold in AUC was observed for MLN3897 in comparison with a predicted value of 3.26-fold. Thus, our model reliably predicted the exposure changes for MLN3897 in interaction studies with competitive CYP3A inhibitors in humans, further strengthening the utility of our in vitro model.

Prediction of clinical DDIs using in vitro studies is one of the major challenges in the pharmaceutical industry. The main utility of such DDI predictions is to help foresee any safety issues anticipated from higher exposures and thus help design clinical trials with better safety. In some instances, clinical DDI studies can be avoided if no significant pharmacokinetic interaction is predicted. Traditionally, DDI predictions have been based on the ratio of the inhibitor concentration [I] and the enzyme inhibition constant K_i ([I]/K_i ratio) (Rostami-Hodjegan and Tucker, 2004; Ito et al., 2004; Obach et al., 2006; 2006 FDA draft guidance on DDI studies at http://WWW.FDA.gov/cder/guidence/6695dft.html). Although this approach had some successes in predicting DDIs, reliability of predictions still remains a challenge (Blanchard et al., 2004; Cook et al., 2004; Ito et al., 2004; Bachmann 2006; Obach et al., 2006). Difficulty remains both in estimating the physiological concentration of the inhibitor at the enzyme site and in reliably determining K_i, which often is affected by the experimental conditions used. Factors such as the protein concentration in the incubation, the substrate of choice, and the enzyme source (Thummel and Wilkinson 1998; Galetin et al., 2006; Lu et al., 2008b) have all been shown to affect the K_i determination. Because the value of [I] (the enzyme site free concentration) cannot be accurately assessed, scientists have used various alternative parameters to investigate what correlated well with in vivo observations for a selection of compounds. The results indicate that no uniform parameter could be used to predict interactions broadly. In our in vitro

Article, publication date, and citation information can be found at http://jpet.aspetjournals.org.
doi:10.1124/jpet.109.161893.

ABBREVIATIONS: DDI, drug-drug interaction; CCR1, C-C chemokine receptor-1; P450, cytochrome P450; fm, fraction of metabolism by a given enzyme; fA, fraction of activity remaining of a given enzyme in the presence of inhibitor; AUC, area under the curve of plasma concentration-time plot; IS, internal standard; QD, once a day; PK, pharmacokinetic; MLN3897, (*S*)-4-(4-chloro-phenyl)-1-{3-[7-(1-hydroxy-1-methyl-ethyl)-11*H*-10-oxa-1-aza-dibenzo[a,d]cyclohepten-(5*E*)-ylidene]-propyl}-3,3-dimethyl-piperidin-4-ol; compound with 3-carboxy-3-hydroxy-pentanedioic acid citrate.

assays, we used human hepatocytes suspended in human plasma, with the plasma concentration of the inhibitors in the incubations being similar to the clinical C_{max} of the inhibitor observed with standard dosing. The free concentration at the enzyme site would be same in the two systems (Lu et al., 2007, 2008a). Consequently, our model eliminates the need to determine the value of [I] and removes the dependence on the traditional, less desirable rule of [I]/K_i ratio to predict magnitude of DDIs.

MLN3897 is a potent and selective antagonist of the C-C chemokine receptor-1 (CCR1). In a preclinical reaction phenotyping study, MLN3897 was determined to be cleared mainly by CYP3A, necessitating the conduct of clinical DDI studies based on the 2006 FDA draft guidance on DDI studies at http://WWW.FDA.gov/cder/guidence/6695dft.html. In the present study, ketoconazole was coadministered with MLN3897 in healthy volunteers to assess the extent of inhibition with a strong CYP3A inhibitor. Fluconazole was then coadministered to evaluate and compare the magnitude of interaction in the presence of a moderate CYP3A inhibitor.

Materials and Methods

Reagents. Pooled human liver microsomes from 50 donors were purchased from XenoTech, LLC (Lenexa, KS). Cryopreserved human hepatocytes were purchased from In Vitro Technologies (Baltimore, MD) and AP Sciences Inc. (Baltimore, MD). 4-Hydroxytolbutamide, 4-hydroxymephenytoin, 1′-hydroxymidazolam, (*S*)-(+)-(*N*)-(3)-benzylnirvanol (benzylnirvanol), and azamulin were purchased from BD Gentest (Woburn, MA). Phenacetin, acetaminophen, tolbutamide, dextromethorphan, dextrorphan, furafylline, sulfaphenazole, quinidine, fluconazole, midazolam, NADPH, and $MgCl_2$ were purchased from Sigma-Aldrich (St. Louis, MO). Human plasma was purchased from Bioreclamation Inc. (Hicksville, NY). (*S*)-Mephenytoin was purchased from BIOMOL Research Laboratories, (Plymouth Meeting, PA). MLN3897 was synthesized at Millennium Pharmaceuticals, Inc. (Cambridge, MA).

P450 Inhibition Determination in Human Hepatocytes. In vitro assays, such as the reaction phenotyping to obtain the relative P450 contribution values (fm) for MLN3897, the determination of P450 activity remaining (fA) in the presence of ketoconazole or fluconazole in human hepatocytes suspended in human plasma, and the calculation of predicted AUC changes from in vitro data were described in our previous reports (Lu et al., 2007, 2008a). In brief, to determine P450 enzyme activity remaining in the presence of inhibitors, the fA values, serially diluted ketoconazole or fluconazole in human plasma was added into human hepatocytes. After allowing 10 min of equilibration time, the P450 isozyme-specific substrates prepared in plasma were added to start 45-min incubations for assessing the P450 activity. The reactions were stopped by adding two volumes of acetonitrile containing 1 μM carbutamide (internal standard). The samples were kept in a refrigerator for 30 min and then centrifuged at 3000*g* for 10 min. The supernatants were analyzed by liquid chromatography-tandem mass spectrometry for the amount of metabolites formed from the probe substrates. The percentage of metabolic activity remaining was calculated by comparing the P450 activities in samples with various concentrations of ketoconazole or fluconazole with their vehicle control. In parallel, extracellular plasma concentrations of ketoconazole or fluconazole were determined after hepatocytes were separated from the plasma using the oil layer separation technique after the 10-min equilibration (Shitara et al., 2003; Lu et al., 2008a). These in vitro extracellular plasma concentrations and their corresponding fA values were used to pair with known clinical plasma C_{max} values to perform DDI prediction.

Reaction Phenotyping of MLN3897 in Human Liver Microsomes Using P450-Selective Chemical Inhibitors. The relative P450 contributions to the hepatic metabolism of MLN3897 (fm) was determined using P450-selective chemical inhibitors. The concentrations of the inhibitor were determined previously in human liver microsomal incubations to produce more selective inhibition of a particular P450, meaning high inhibition toward the target P450 but less of cross-inhibition to other P450s. P450 probe substrates were also incubated in the study to determine the partial inhibition and cross reactivity of these inhibitors. The results from P450 probe substrate incubations were then used to calculate the inhibition of MLN3897 metabolism, assuming that it is subject to same degree of partial inhibition and cross-reactivity to these inhibitors as the probe substrates (Lu et al., 2007). Specifically, human liver microsomes (25 μl; final concentration of 0.5 mg/ml in 0.1 M potassium phosphate buffer, pH 7.4) were prewarmed in 96-well plates for 5 min at 37°C, in duplicate, with 25 μl of MLN3897 or probe substrates (at their respective K_m concentrations) and 25 μl of P450-selective inhibitors prepared in the same buffer. The reactions were initiated by the addition of 25 μl of NADPH/$MgCl_2$ in 0.1 M potassium phosphate buffer (final concentration of 2 and 3 mM, respectively) and incubated for 15 min. Acetonitrile (1%, final concentration) and dimethyl sulfoxide (0.1%) were used as solvent to increase compound solubility, and they have minimal effect on P450 activity. The reactions were terminated by the addition of 100 μl of acetonitrile containing 1 μM carbutamide as the internal standard (IS). After storing for 30 min in a refrigerator, the sample plates were centrifuged at 3000*g* for 10 min, and the supernatants were analyzed using liquid chromatography-mass spectrometry. The final concentrations of the respective P450-selective inhibitors and probe substrates were as follows: 100 μM furafylline and 30 μM phenacetin for CYP1A2; 5 μM sulfaphenazole and 150 μM tolbutamide for CYP2C9; 20 μM benzylnirvanol and 100 μM (*S*)-mephenytoin for CYP2C19; 5 μM quinidine and 8 μM dextromethorphan for CYP2D6; and 2 μM azamulin and 50 μM testosterone for CYP3A4. The method for calculation of AUC changes from the in vitro data (predicted DDI) using the equation shown under *Results* was described previously (Lu et al., 2007).

Effect of Ketoconazole on Steady-State Pharmacokinetics of MLN3897. The ketoconazole and fluconazole-MLN3897 clinical DDI studies were carried out in accordance with the good clinical practice principles enunciated in the Declaration of Helsinki (revised version of Edinburgh, Scotland, 2000; Note of Clarification on Paragraph 29 added by the World Medical Association General Assembly, Washington, 2002), and the International Conference on Harmonisation harmonized tripartite guideline regarding good clinical practice (E6 Consolidated Guidance, April 1996). The study was approved by the Institutional Review Board, and informed consent was obtained for each subject.

Because of the long plasma half-life of MLN3897, it was administered orally at a proposed efficacious dose of 10 mg once a day (QD) to 20 healthy subjects (10 males and 10 females), for 16 consecutive days (greater than five half-lives) (Fig. 1) to reach steady state. The mean age, height, and weight was 28 years, 171.3 cm, and 70.5 kg, respectively. The PK profile was measured on day 16. After a washout period (days 17–33), ketoconazole was administered at 200 mg b.i.d. from day 34 through day 58. MLN3897 coadministration was started on day 37 and continued through day 58. The extended dosing for MLN3897 (compared with period 1; 16 days preketoconazole dosing versus 22 days with ketoconazole) was to ensure achievement of a new steady state, accounting for the anticipated increase in half-life of MLN3897 when coadministered with P450 inhibitor ketoconazole. On day 58, the PK of MLN3897 was measured again. The ratio of AUC of MLN3897 administrated with ketoconazole over MLN3897 alone was calculated.

Effect of Fluconazole on Steady-State Pharmacokinetics of MLN3897 and Effect of MLN3897 on CYP3A Activity. A slightly modified study design was applied for the fluconazole DDI trial with 17 healthy subjects (11 males, 6 females; Fig. 2). The mean age, height, and weight was 33 years, 171.7 cm, and 74.6 kg, respectively. Because MLN3897 was tolerated at higher exposure when coadmin-

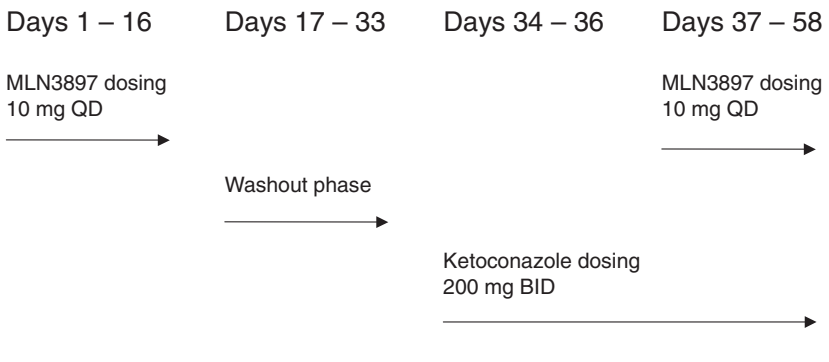

Fig. 1. MLN3897 and ketoconazole clinical drug-drug interaction study dosing schedule. MLN3897 PK profiles were measured on days 16 and 58.

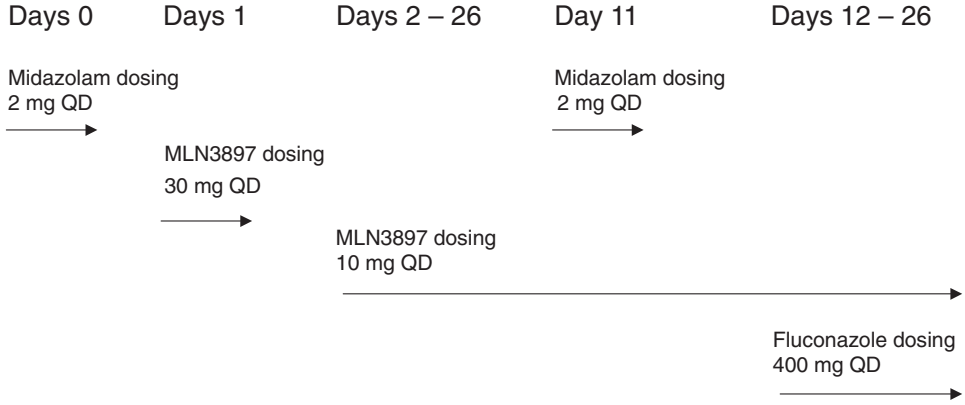

Fig. 2. MLN3897 and fluconazole clinical drug-drug interaction study dosing schedule. Thirty milligrams of loading dose was given on day 1. MLN3897 PK profiles were measured on days 10 and 26.

istered with ketoconazole, on day 1, a calculated, loading dose of 30 mg QD of MLN3897 was given orally followed by 25 additional doses of 10 mg QD of MLN3897. The pharmacokinetics was measured on day 10. Fluconazole at 400 mg QD was then administered along with 10 mg of MLN3897 from day 12 to day 26. The PK of MLN3897 with coadministration of fluconazole was measured again on day 26, and the AUC ratio was determined to assess the magnitude of the DDI.

An initial part of this study had been constructed to evaluate whether MLN3897 had any effect on CYP3A activities. MLN3897, maintained at steady-state levels, and midazolam (2 mg QD), a selective CYP3A substrate, were concurrently dosed orally on day 0 (pre-MLN3897 dose) and day 11, and the PK profiles were compared.

Clinical Plasma Sample Analysis. Blood samples were collected at various time points and centrifuged at approximately 2500 rpm for approximately 15 min at 4°C to obtain plasma samples. Plasma samples were stored at or below −80°C within 1 h of collection. Samples were assayed for MLN3897 under good laboratory practice using a validated liquid chromatography coupled with tandem mass spectrometry method. Specifically, plasma samples (100 μl) were processed using a liquid-liquid extraction procedure to isolate the analyte and the IS MLN3897-d6 from human plasma. The extracted samples were dried, reconstituted in 100 μl of 50:50 mixture of acetonitrile and 5 mM ammonium hydroxide, and 15 μl of the reconstituted solution was injected onto a Zorbax Extend-C18 column (2.1 × 100 mm; 3.5 μm) for analysis. The high-performance liquid chromatography separation was performed at a flow of 0.3 ml/min under a gradient elution mode with 5 mM ammonium hydroxide in water as mobile phase A and acetonitrile as mobile phase B. Each gradient analysis took approximately 4 min. The mass transitions used were *m/z* 533.4 → 236.3 for MLN3897 and *m/z* 539.4 → 236.3 for the IS. The dynamic range of the assay was 0.05 to 50 ng/ml. Plasma concentrations below the lower limit of quantification were treated as 0 ng/ml for calculation of summary statistics. Plasma concentrations above the upper limit of detection were reassayed after dilution for the concentrations to fall within the dynamic range of the assay.

Results

The CYP3A inhibition and cross-inhibition for CYP1A2, CYP2C9, CYP2C19, CYP2D6, and CYP3A4 by ketoconazole and fluconazole in human hepatocytes suspended in human plasma are presented in Tables 1 and 2 as a fraction of the activity remaining (fA). The relative contribution of the above-mentioned five major P450s toward the hepatic metabolism (fm) of MLN3897 is presented in Table 3. MLN3897 is mainly cleared via hepatic metabolism (i.e., $f_{m,hep} = 1$), with negligible renal clearance (data not shown). The DDI prediction method described previously (Lu et al., 2007) involved two in vitro parameters, fA_{CYP} and fm_{CYP}, linked using the following equation:

$$\frac{AUC_1}{AUC} = \frac{CL}{CL_1} = \frac{1}{f_{m,hep}(fm_{3A4}fA_{3A4} + fm_{2C9}fA_{2C9} + \ldots) + f_{other}fA_{other}}$$

where $f_{m,hep}$ is the fraction of clearance by hepatic metabolism, $f_{m,cyp}$ is the relative contribution of an individual P450 to the total metabolism of the compound (without inhibitor), and fA_{CYP} is the fraction of enzyme activity remaining in the presence of the inhibitor. f_{other} is the fraction of clearance by other routes such as renal or biliary excretion ($f_m + f_{other} = 1$). Experimental or clinical information of the effects of the inhibitor on the bioavailability across gastrointestinal tract (Fg'/Fg) are generally not available (Galetin and Houston, 2009); therefore, this term was not included in our calculations. To assess the worst-case scenario of interaction, the clinical maximum plasma concentration of the inhibitor (C_{max}) was used to calculate the fA values. With these two simplifications, the latter step may compensate for the

TABLE 1

P450 activity remaining in human hepatocytes in the presence of ketoconazole in human plasma

Ketoconazole was equilibrated with human hepatocytes in human plasma to allow nonspecific binding. After equilibration, the extracellular concentration of ketoconazole was measured. The remaining P450 activities in hepatocytes (fA) were also determined using the probe substrates. Table adapted from Lu et al. (2007).

Keto in Incubation	Keto Extracellular	CYP1A2	CYP2C9	CYP2C19	CYP2D6	CYP3A4
	μM			*fA (%)*[a]		
100 μM	71.8	79	60	32	96	0
50 μM	34.0	81	71	42	84	0
25 μM	14.1	83	72	57	99	0
12.5 μM	7.30	89	75	63	91	1
6.25 μM	4.04	92	80	83	99	5
3.13 μM	2.22	92	84	90	100	11
1.6 μM	0.857	97	79	89	97	12
0 μM	0	100	100	100	100	100

Keto, ketoconazole.
[a] fA (%), fraction of enzyme activity remaining in the presence of ketoconazole inhibition.

TABLE 2

Effect of fluconazole on P450 activity remaining in human hepatocytes suspended in human plasma

Fluconazole was equilibrated with human hepatocytes in human plasma to allow nonspecific binding. After equilibration, the extracellular concentration of fluconazole was measured. The remaining P450 activities in hepatocytes (fA) were also determined using the probe substrates. Adapted from Lu et al. (2008a).

Total Fluconazole in Incubation	Fluconazole Extracellular	CYP1A2	CYP2C9	CYP2C19	CYP2D6	CYP3A4
	μM			*fA (%)*[a]		
100 μM	98.4	91.9	21.2	10.6	74.2	15.4
50 μM	47.2	112	36.8	14.9	97.6	23.3
25 μM	26.5	89.5	55.2	27.8	102	34.9
12.5 μM	13.1	97.5	66.3	45.2	87.4	39.8
6.25 μM	6.10	90.8	78.9	64.7	115	50.6
3.13 μM	3.13	85.1	86.7	75.7	110	59.9
1.57 μM	1.46	90.0	89.3	89.2	89.0	66.7
0 μM	0	100	100	100	100	100

[a] fA (%), fraction of enzyme activity remaining in the presence of fluconazole inhibition.

TABLE 3

Relative contributions of CYP1A2, CYP2C9, CYP2C19, CYP2D6, and CYP3A4 to the metabolism of MLN3897 in human liver microsomes

	P450				
	2C9	1A2	2C19	2D6	3A4
Fm (%)[a]	0	4.8	0	21	87

[a] fm (%), fractional contribution of specific P450s to the metabolism of MLN3897.

former. Using this model, the predicted AUC increases of MLN3897 with ketoconazole (200 mg b.i.d.) and fluconazole (400 mg QD) at steady state were 8.33- and 3.26-fold, respectively.

Figure 3 shows the steady-state mean plasma concentration increase of MLN3897 in both male and female subjects (total $n = 20$) before and after multiple days of treatment with 200 mg b.i.d. of ketoconazole. There was little difference between the concentration-time profiles in male and female subjects, in agreement with the literature that gender differences in humans are minimal (Greenblatt and von Moltke, 2008). However, an over 8-fold increase in MLN3897 AUC was observed in both groups, relative to their MLN3897 given alone groups. Figure 4 presents the daily trough concentration of MLN3897 with and without coadministration of ketoconazole. The data show MLN3897 reaches steady-state concentrations in 10 to 14 days, and longer time is required after ketoconazole coadministration. Table 4 summarizes the main pharmacokinetic parameters. Upon coadministration with ketoconazole, increases in AUC, C_{max}, and C_{min} at the steady state were 8.28-, 7.39-, and 9.27-fold, respectively. Figure 5 presents the individual AUC increases upon coadministration for the 20 subjects. The AUC change ranged from 4.5- to 13.0-fold.

A summary of the main pharmacokinetics parameters for the MLN3897-fluconazole DDI study ($n = 17$) is shown in Table 5. The mean MLN3897 AUC change upon coadministration of fluconazole was 3.93-fold with individual variation from 2.5- to 7.3-fold. The increase of C_{max} and C_{min} at the steady state was at the similar level (3.51- and 4.98-fold, respectively). The PK profile of MLN3897 at steady state before and after coadministration of fluconazole is shown in Fig. 6.

Part of this clinical DDI study is designed to access whether repeated dosing of MLN3897 would affect the CYP3A activity. The PK profiles (data not shown) of midazolam pre- and post-MLN897 treatment showed no CYP3A activity change, as expected. Because the evaluation of MLN3897 as a perpetrator of CYP3A-mediated DDI is not the focus of this article, no further discussion is included.

Discussion

The primary objectives of this study were to investigate the potential CYP3A inhibitor-mediated DDI risk for an investigational CCR1 antagonist and CYP3A substrate MLN3897 in healthy volunteers and to demonstrate an in vitro-in vivo correlation using a recently proposed novel in vitro prediction model (Lu et al., 2007, 2008a,b). In our DDI prediction model, inhibitors such as ketoconazole or fluconazole were incubated with human hepatocytes in 100% human plasma to construct concentration-P450 inhibition titration curves under conditions closely resembling those in vivo. At equilibrium, the extracellular (plasma) concentrations of the inhibitor were measured after separating the plasma from hepatocytes. Matching the extracellular plasma concentration in vitro with the plasma C_{max} found in in vivo study then provided the extent of inhibition of various P450s from the titration

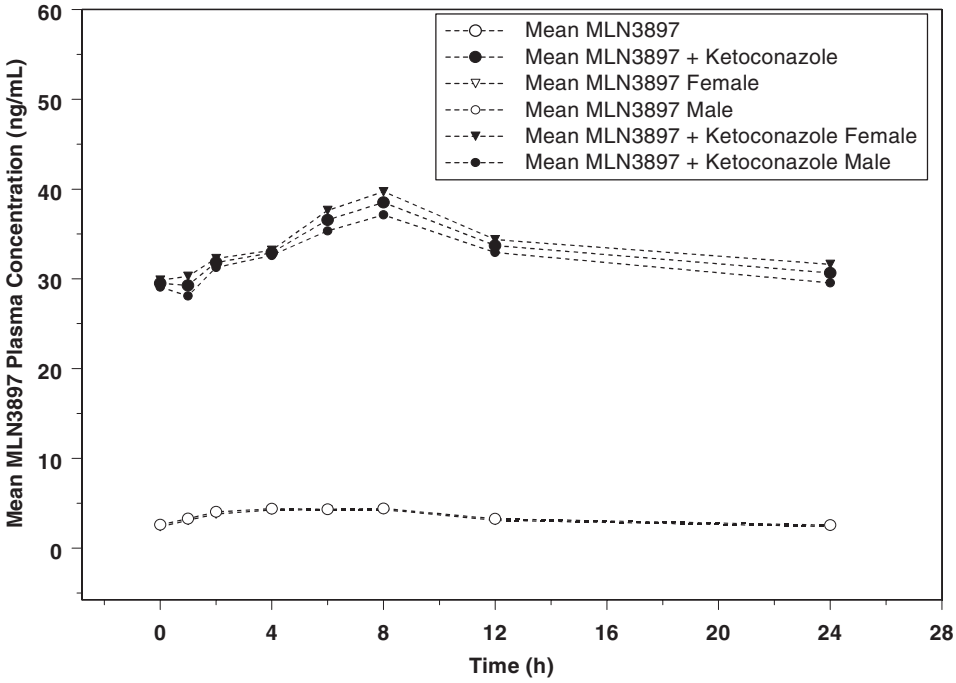

Fig. 3. Mean plasma concentration versus time profile after a 10-mg dose of MLN3897 and MLN3897 + ketoconazole.

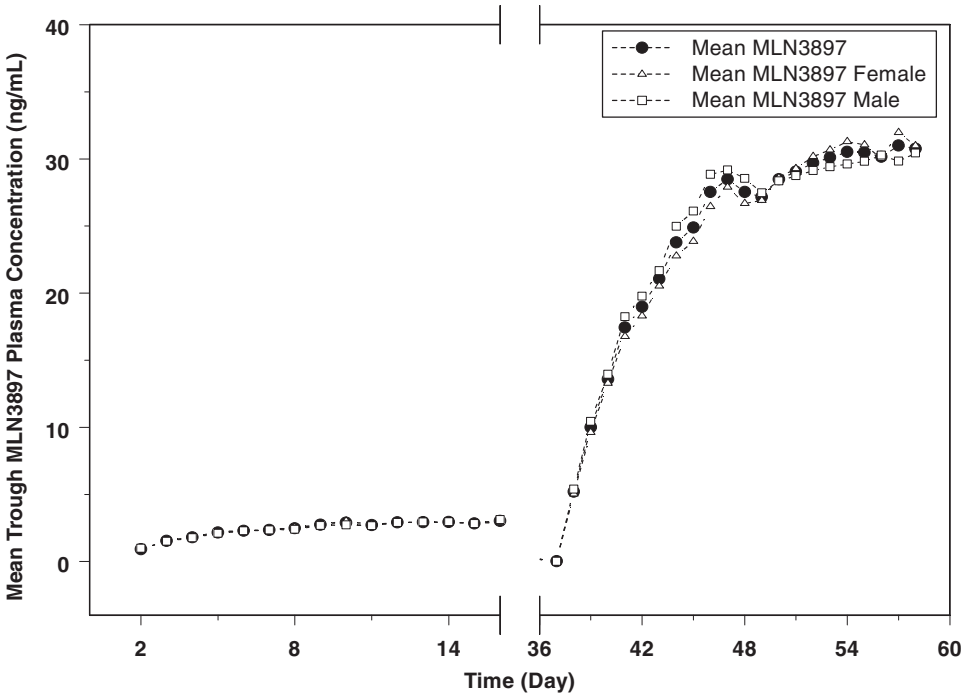

Fig. 4. Mean trough plasma concentration versus time profile after 10-mg dose of MLN3897 and MLN3897 + ketoconazole.

TABLE 4
Summary of the plasma pharmacokinetic parameters of MLN3897 for treatments with and without ketoconazole
Data are mean ± S.D.

Pharmacokinetic Parameter	MLN3897 + Ketoconazole	MLN3897	Fold Change
AUC_{0-24} (ng · h/ml)	830.6 ± 236.3	100.3 ± 60.5	8.28
T_{max} (h)	7.99	6.01	1.33
C_{max}ss (ng/ml)	40.8 ± 11.7	5.52 ± 3.17	7.39
C_{min}ss (ng/ml)	29.4 ± 8.9	3.17 ± 2.14	9.27

curves. This avoided the need to use the $[I]/K_i$ ratio approach for DDI predictions. Essentially, the free concentrations at the enzyme site in vitro and in vivo would be comparable, and so would the extent of inhibition. This model has been validated with 15 marketed drugs with ketoconazole ($r^2 = 0.97$ for the in vitro-in vivo correlation; Lu et al., 2008a). A similar approach was applied to fluconazole with nine marketed drugs, where a good DDI prediction was demonstrated, with $r^2 = 0.71$ (Lu et al., 2008b).

Three parameters used in this model are $f_{m,hep}$, fm_{CYP}, and fA_{CYP}. The $f_{m,hep}$ is considered to be unity based on the

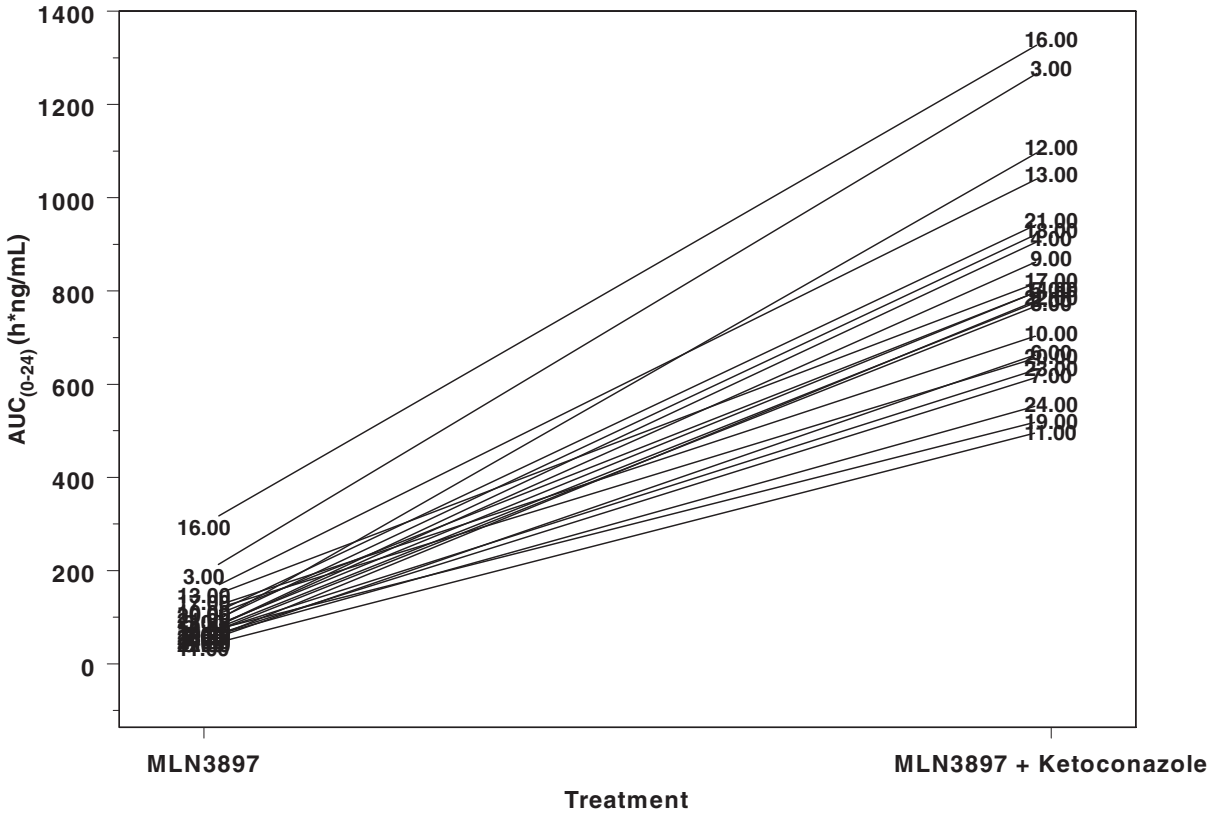

Fig. 5. AUC_{0-24h} increase after coadministration of MLN3897 and ketoconazole among 20 healthy volunteers.

TABLE 5
Summary of the plasma pharmacokinetic parameters of MLN3897 for treatments with and without fluconazole
Data are mean ± S.D.

Pharmacokinetic Parameter	MLN3897 + Fluconazole	MLN3897	Fold Change
AUC_{0-24} (ng · h/ml)	327.3 ± 115.3	83.3 ± 35.2	3.93
T_{max} (h)	8.00	6.55	1.22
C_{max}ss (ng/ml)	16.3 ± 6.1	4.64 ± 1.97	3.51
C_{min}ss (ng/ml)	11.0 ± 4.2	2.21 ± 1.02	4.98

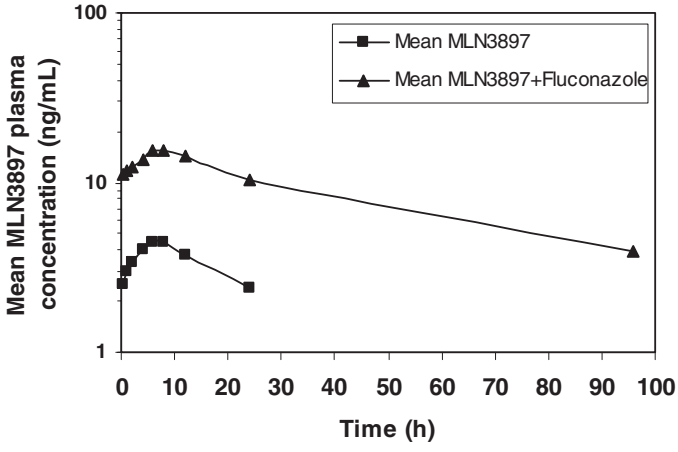

Fig. 6. Mean trough plasma concentration versus time profile following 10-mg dose of MLN3897 and MLN3897 + fluconazole.

human absorption, distribution, metabolism, and excretion study, where MLN3897 was cleared mainly through metabolism. The fm_{CYP} was determined by quantitative P450 phenotyping. As discussed previously (Lu et al., 2007), fA was calculated by intrapolation of the two closely measured fA values from the inhibition titration curves in hepatocyte incubations, covering the in vivo C_{max} value of the inhibitor. For the model, at the reported C_{max} of 10 μM ketoconazole after 200 mg b.i.d. (Pelkonen et al., 1998), the fA values for CYP1A2, CYP2C9, CYP2C19, and CYP3A4 were calculated to be 0.864, 0.739, 0.604, and 0.006, respectively. CYP2D6 was not inhibited by ketoconazole at physiologically relevant concentrations. For fluconazole, at the reported C_{max} of 69.2 μM at 400-mg QD dose (Brunton et al., 2006), the fA values were calculated to be 0.308, 0.133, and 0.203 for CYP2C9, CYP2C19, and CYP3A4, respectively. CYP1A2 and CYP2D6 were not inhibited by fluconazole.

MLN3897 is being investigated for chronic oral administration to treat inflammatory diseases. To assess the maximal effect of CYP3A inhibition on MLN3897, administration of MLN3897 until steady state was reached was necessary. Because MLN3897 has a half-life of approximately 3 to 4 days, the steady state was expected in 16 days (four to five half-lives). In the presence of an inhibitor, the half-life of MLN3897 was expected to be prolonged; therefore, the coadministration of MLN3897 and ketoconazole was extended out to 22 days to ensure achievement of steady state. A similar time frame was applied for a washout period.

Coadministration of the CYP3A substrate MLN3897 with a strong CYP3A inhibitor, ketoconazole, resulted in the predicted elevation (8.33-fold; as predicted from the in vitro model) of steady-state MLN3897 AUC and represents the most extreme inhibition likely to be seen with clinically used CYP3A inhibitors. Fluconazole is a moderate CYP3A inhibitor and also inhibits other P450s, such as CYP2C9 and CYP2C19 (Venkatakrishnan et al., 2000). The DDI study

using fluconazole illustrates what would be expected when a moderate CYP3A inhibitor is used with MLN3897 (which has no CYP2C9 or CYP2C19 contributions to its clearance). Because the observed greater than 8-fold elevation of exposure to MLN3897 was well tolerated in healthy subjects, a loading dose design was applied in the MLN3897-fluconazole DDI study to reduce the study time needed to reach the steady state. The pharmacokinetic parameters of MLN3897 determined after administration of a 30-mg loading dose of MLN3897, followed by 10 mg QD administration of MLN3897 over 10 days were comparable with those observed in the ketoconazole study. The AUC increase of MLN3897 with fluconazole was 3.93-fold, an increase closely predicted (3.26-fold) by our in vitro model.

In summary, the clinical drug interaction studies of MLN3897 with ketoconazole and fluconazole yielded exposure increases for MLN3897, at steady state, that were predicted closely by our in vitro model. The model is not dependent on the traditional, ambiguous, and unreliable $[I]/K_i$ method. The DDI study for fluconazole was an "adaptive" design based on ketoconazole data, and allowed subjects to reach the steady state faster through the safe use of a loading dose. The predicted power of this simple in vitro model is further validated by the current studies. Such dependable predictions are expected to benefit clinical trials because any increased pharmacodynamic or side effects that are linked to pharmacokinetics can be anticipated. If necessary, doses can be adjusted to stay within a desired plasma range.

References

Bachmann KA (2006) Inhibition constants, inhibitor concentrations and the prediction of inhibitory drug drug interactions: pitfalls, progress and promise. *Curr Drug Metab* **7:**1–14.

Blanchard N, Richert L, Coassolo P, and Lavé T (2004) Qualitative and quantitative assessment of drug-drug interaction potential in man, based on Ki, IC_{50} and inhibitor concentration. *Curr Drug Metab* **5:**147–156.

Brunton LL, Lazo JS, and Park KL (2006) *Goodman & Gilman's The Pharmacocological Basis of Therapeutics*, McGraw-Hill, New York.

Cook CS, Berry LM, and Burton E (2004) Prediction of in vivo drug interactions with eplerenone in man from in vitro metabolic inhibition data. *Xenobiotica* **34:**215–228.

Galetin A and Houston JB (2009) Inhibition of drug metabolism enzymes in gastrointestinal tract and its influence on the drug-drug interaction prediction, in *Enzyme Inhibition in Drug Discovery and Development: The Good and the Bad* (Lu C and Li AP eds) pp 519–557, Wiley Press, Hoboken, NJ.

Galetin A, Ito K, Hallifax D, and Houston JB (2006) CYP3A4 substrate selection and substitution in the prediction of potential drug-drug interaction prediction, *J Pharmacol Exp Ther* **314:**180–190.

Greenblatt DJ and von Moltke LL (2008) Gender has a small statistically significant effect on clearance of CYP3A substrate drugs. *J Clin Pharmacol* **48:**1350–1355.

Ito K, Brown HS, and Houston JB (2004) Database analyses for the prediction of in vivo drug-drug interactions from in vitro data. *Br J Clin Pharmacol* **57:**473–486.

Lu C, Berg C, Prakash SR, Lee FW, and Balani SK (2008a) Prediction of pharmacokinetic drug-drug interactions using human hepatocyte suspension in plasma and cytochrome P450 phenotypic data. III. In vitro-in vivo correlation with fluconazole. *Drug Metab Dispos* **36:**1261–1266.

Lu C, Hatsis P, Berg C, Lee FW, and Balani SK (2008b) Prediction of pharmacokinetic drug-drug interactions using human hepatocyte suspension in plasma and cytochrome P450 phenotypic data. II. In vitro-in vivo correlation with ketoconazole. *Drug Metab Dispos* **36:**1255–1260.

Lu C, Miwa GT, Prakash SR, Gan LS, and Balani SK (2007) A novel model for the prediction of drug-drug interactions in humans based on in vitro cytochrome P450 phenotyping data. *Drug Metab Dispos* **35:**79–85.

Obach RS, Walsky RL, Venkatakrishnan K, Gaman EA, Houston JB, and Tremaine LM (2006) The utility of in vitro cytochrome P450 inhibition data in the prediction of drug-drug interactions. *J Pharmacol Exp Ther* **316:**336–348.

Pelkonen O, Mäenpää J, Taavitsainen P, Rautio A, and Raunio H (1998) Inhibition and induction of human cytochrome P450 (CYP) enzymes. *Xenobioteca* **28:**1203–1253.

Rostami-Hodjegan A and Tucker GT (2004) "In silico" simulation to assess the "in vivo" consequences of "in vitro" metabolic drug-drug interactions. *Drug Discov Today Tech* **1:**441–448.

Shitara Y, Li AP, Kato Y, Lu C, Ito K, Itoh T, and Sugiyama Y (2003) Function of uptake transporters for taurocholate and estradiol 17beta-D-glucuronide in cryopreserved human hepatocytes. *Drug Metab Pharmacokinet* **18:**33–41.

Thummel KE and Wilkinson GR (1998) In vitro and in vivo drug interactions involving human CYP3A. *Annu Rev Pharmacol Toxicol* **38:**389–430.

Venkatakrishnan K, von Moltke LL, and Greenblatt DJ (2000) Effects of the antifungal agents on oxidative drug metabolism: clinical relevance. *Clin Pharmocokinet* **38:**111–180.

Address correspondence to: Dr. Chuang Lu, Millennium Pharmaceuticals, Inc., 40 Landsdowne St., Cambridge, MA 02139. E-mail: chuang.lu@mpi.com